

# UCLA

## UCLA Previously Published Works

### Title

Efficient Dielectrophoretic Patterning of Embryonic Stem Cells in Energy Landscapes Defined by Hydrogel Geometries

### Permalink

<https://escholarship.org/uc/item/7cc0c97j>

### Journal

Annals of Biomedical Engineering: The Journal of the Biomedical Engineering Society, 38(12)

### ISSN

1573-9686

### Authors

Tsutsui, Hideaki  
Yu, Edmond  
Marquina, Sabrina  
et al.

### Publication Date

2010-12-01

### DOI

10.1007/s10439-010-0108-1

Peer reviewed

# Efficient Dielectrophoretic Patterning of Embryonic Stem Cells in Energy Landscapes Defined by Hydrogel Geometries

HIDEAKI TSUTSUI,<sup>1</sup> EDMOND YU,<sup>1</sup> SABRINA MARQUINA,<sup>1</sup> BAHRAM VALAMEHR,<sup>2</sup> IEONG WONG,<sup>1</sup>  
HONG WU,<sup>2</sup> and CHIH-MING HO<sup>1</sup>

<sup>1</sup>Department of Mechanical and Aerospace Engineering, University of California, Los Angeles, Los Angeles, CA 90095, USA; and <sup>2</sup>Department of Molecular and Medical Pharmacology, University of California, Los Angeles, Los Angeles, CA 90095, USA

(Received 21 January 2010; accepted 18 June 2010; published online 8 July 2010)

Associate Editor Michael S. Detamore oversaw the review of this article.

**Abstract**—In this study, we have developed an integrated microfluidic platform for actively patterning mammalian cells, where poly(ethylene glycol) (PEG) hydrogels play two important roles as a non-fouling layer and a dielectric structure. The developed system has an embedded array of PEG microwells fabricated on a planar indium tin oxide (ITO) electrode. Due to its dielectric properties, the PEG microwells define electrical energy landscapes, effectively forming positive dielectrophoresis (DEP) traps in a low-conductivity environment. Distribution of DEP forces on a model cell was first estimated by computationally solving quasi-electrostatic Maxwell's equations, followed by an experimental demonstration of cell and particle patterning without an external flow. Furthermore, efficient patterning of mouse embryonic stem (mES) cells was successfully achieved in combination with an external flow. With a seeding density of  $10^7$  cells/mL and a flow rate of 3  $\mu$ L/min, trapping of cells in the microwells was completed in tens of seconds after initiation of the DEP operation. Captured cells subsequently formed viable and homogeneous monolayer patterns. This simple approach could provide an efficient strategy for fabricating various cell microarrays for applications such as cell-based biosensors, drug discovery, and cell microenvironment studies.

**Keywords**—Poly(ethylene glycol), Surface engineering, Cell microarray, Microfluidics, Dielectrophoresis.

## INTRODUCTION

Surface-patterned cell arrays are indispensable platforms for cell-based sensors,<sup>5,12</sup> drug discovery,<sup>9</sup> as well as investigating cell–cell or cell–matrix inter-

actions in a well-controlled manner *in vitro*.<sup>13,41</sup> Advances in surface chemistry and material sciences in conjunction with developments of micro/nano fabrication techniques have led to various methods of cellular patterning,<sup>12,13,32,44</sup> including, but not limited to, photolithography,<sup>6,19,20,25,33</sup> microcontact printing,<sup>7,36</sup> micromolding,<sup>22,37</sup> stencil patterning,<sup>14,39</sup> microchannel patterning,<sup>23,38</sup> and inkjet printing.<sup>34,35</sup> The majority of such cellular patterning methods rely on spatially defined so-called non-fouling surfaces on a substrate (e.g., glass, silicon, and polystyrene plate), to which non-specific binding of protein components from cell culture media is significantly reduced or eliminated, compared with unmodified surfaces. A sequence of coating with cell-adhesive molecules such as extracellular matrix (ECM) proteins, charged polymers, or antibodies, washing off the adhesive components from the non-fouling areas, incubating with target cells, and carefully rinsing to remove excess cells leads to defined patterns of the cells on a fabricated substrate. Such surface-based cell patterning is passive in nature and has several drawbacks; (a) settlement of cells takes a few hours, (b) falling of cells is a stochastic process, leading to non-uniform cell distributions, (c) the majority of cells falling onto non-fouling surface are wasted, and (d) developing clean patterns of cells usually requires extremely careful washing.

Dielectrophoresis (DEP) is the motion of a polarizable particle induced by non-uniform electric fields,<sup>21,30</sup> and has been frequently employed in cell and particle separation/sorting in microfluidic systems.<sup>29,40</sup> Recently, DEP forces generated by a patterned microelectrode array were used to actively pattern bovine pulmonary arterial endothelial cells on the trapping electrodes.<sup>16</sup> In this study, the DEP

Address correspondence to Chih-Ming Ho, Department of Mechanical and Aerospace Engineering, University of California, Los Angeles, Los Angeles, CA 90095, USA. Electronic mail: chihming@ucla.edu

patterning demonstrated significantly more accurate patterning of cells on desired spots compared with poor patterning via conventional surface modification methods, while not compromising viability and growth of the patterned cells. In other studies, a layer of an electrically insulating photoresist was patterned on a planar electrode to create a virtual electrode array for temporal cell trapping and subsequent encapsulation in a hydrogel.<sup>1,2</sup> As demonstrated in these studies, insulating materials can be used to shape highly non-uniform electric fields required for DEP manipulation (insulator-based DEP) of cells and particles,<sup>11</sup> while significantly simplifying the fabrication process and improving ease of operations. However, commonly used insulating polymer materials such as SU-8 and polydimethylsiloxane (PDMS) do not have good non-fouling characteristics and inefficiently prevent non-specific binding of protein components as well as cell attachment and growth. Therefore, it is highly desired that the insulating layer is made of non-fouling materials for improved fidelity and long-term stability of the defined cell patterning. Here we propose to develop a quick (~tens of seconds) and active cell patterning method based on positive dielectrophoretic (DEP) traps, which are defined by non-fouling microwell structures made of poly(ethylene glycol) (PEG) hydrogels.

## THEORY

The time-averaged DEP force  $\mathbf{F}_{\text{DEP}}$  on a particle of radius  $r$ , imposed by an AC electric field  $\mathbf{E}$  of angular frequency  $\omega$ , is given as<sup>21,43</sup>:

$$\mathbf{F}_{\text{DEP}} = 2\pi\epsilon_m r^3 \text{Re}[f_{\text{CM}}] \nabla |\mathbf{E}_{\text{rms}}|^2 \quad (1)$$

where  $\epsilon_m$  is the permittivity of the surrounding medium, and  $f_{\text{CM}}$  is the Clausius–Mossotti (CM) factor defined as:

$$f_{\text{CM}} = \frac{\epsilon_p^* - \epsilon_m^*}{\epsilon_p^* + 2\epsilon_m^*}. \quad (2)$$

Here  $\epsilon_p^*$  and  $\epsilon_m^*$  are the complex permittivities of the particle and the surrounding medium, respectively. Each complex permittivity takes the form  $\epsilon^* = \epsilon - j\sigma/\omega$ , where  $\epsilon$  and  $\sigma$  are the permittivity and electrical conductivity of the corresponding substances, respectively.  $j = \sqrt{-1}$  is the imaginary unit. The real part of the CM factor,  $\text{Re}[f_{\text{CM}}]$ , dictates the direction and relative strength of the DEP force in a given electric field; when it is positive the particle is pulled toward a higher electric field region (positive DEP), whereas when negative the particle is pulled away from a higher electric field region (negative DEP).

According to Eq. 1 the DEP force is proportional to  $\nabla |\mathbf{E}_{\text{rms}}|^2$ , meaning that non-uniformity but not mere magnitude of the electric field is critical for generating substantial DEP forces. In this study, we use dielectric microwell structures made of a non-fouling PEG hydrogel to create such a non-uniform electric field (Fig. 1). Under current experimental conditions with a small length scale (~100  $\mu\text{m}$ ) and a moderate AC frequency (~10 MHz), quasi-electrostatic estimation of the time-varying electric field can be applied. Therefore, we solved quasi-electrostatic Maxwell's equations given as<sup>17</sup>:

$$\begin{aligned} \mathbf{E} &= -\nabla\phi \\ \nabla \cdot \mathbf{J} + \frac{\partial \rho}{\partial t} &= 0 \\ \nabla \cdot \mathbf{D} &= \rho \end{aligned} \quad (3)$$

where  $\phi$  is the electric potential,  $\mathbf{J}$  is the current vector,  $\rho$  is the free charge density, and  $\mathbf{D}$  is the electric flux density. Considering  $\mathbf{J} = \sigma\mathbf{E}$  and  $\mathbf{D} = \epsilon\mathbf{E}$  for a homogeneous linear dielectric substance, Eq. 3 is combined to result in:

$$\nabla \cdot (\sigma\nabla\phi) + \frac{\partial}{\partial t}(\nabla \cdot (\epsilon\nabla\phi)) = 0. \quad (4)$$

By introducing a phasor  $\tilde{\phi}(x, t) = (\phi_R + j\phi_I)e^{j\omega t}$ , Eq. 4 reduces to Laplace's equation for the real and imaginary parts of the phasor,

$$\begin{aligned} \nabla^2 \phi_R &= 0 \\ \nabla^2 \phi_I &= 0. \end{aligned} \quad (5)$$

Equation 5 can be solved numerically for a model 2-D space with boundary conditions described in Fig. 2. The electric field is then calculated from Eq. 6 and used to estimate available DEP force in Eq. 1.

$$\mathbf{E} = \text{Re}[-\nabla\tilde{\phi}] = \text{Re}[-\nabla(\phi_R + j\phi_I)e^{j\omega t}] \quad (6)$$

## MATERIALS AND METHODS

### Materials

Poly(ethylene glycol) diacrylate (PEG-DA, Mn ~ 258), 2,2-Dimethoxy-2-phenylacetophenone (DMPA), 3-(Trimethoxysilyl)propyl acrylate (TPA), ethanol, toluene, triethylamine, HEPES, calcium chloride, D-glucose, sucrose, sodium hydroxide, saponin,  $\beta$ -mercaptoethanol, and gelatin were purchased from Sigma-Aldrich (St. Louis, MO). (Tridecafluoro-1,1,2,2-tetrahydrooctyl) trichlorosilane, vinyltrimethoxysilane and 10-undecenyl trimethoxysilane were purchased from Gelest (Morrisville, PA). Indium tin

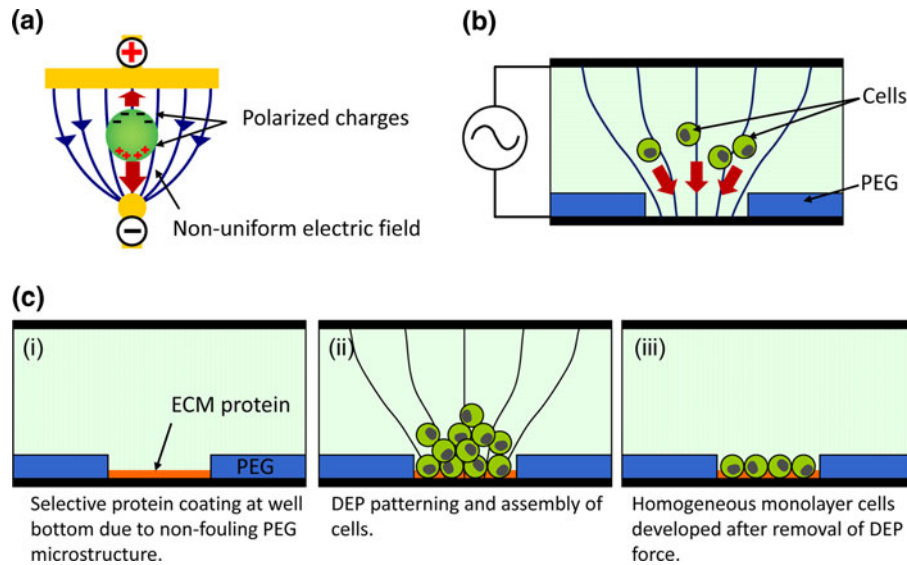


**FIGURE 1.** Proposed cell patterning method using positive DEP force defined by non-fouling microstructures. (a) Positive DEP by metal electrodes; electrical interaction between a non-uniform electric field and polarized charges induced by the field exerts a net force on the particle toward a higher electric field region. (b) Dielectric properties of PEG microstructures can be used to generate a non-uniform electric field required for positive DEP manipulation of mammalian cells. (c) A three-step approach for efficient patterning of cells. (c-i) Non-fouling property of PEG allows for selective coating of ECM proteins in the microwell. (c-ii) cells are attracted to the microwells due to positive DEP forces. (c-iii) After removal of electrical potential and gentle washing, excess cells are removed to reveal a monolayer of patterned cells.

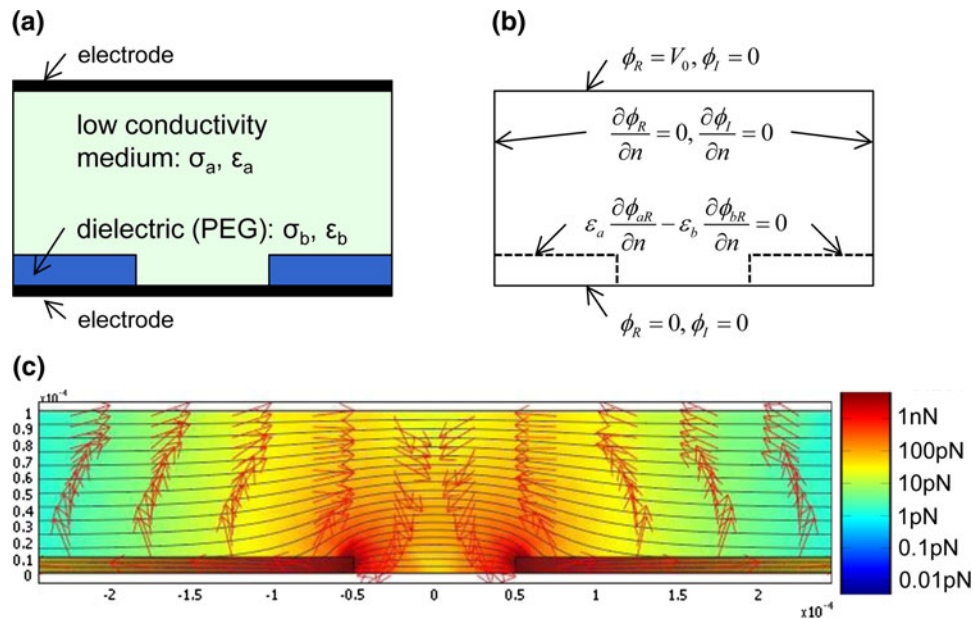


**FIGURE 2.** Finite element analysis of positive DEP force on a mammalian cell. (a, b) Computational domain ( $1000 \mu\text{m} \times 100 \mu\text{m}$ ) and boundary conditions for solving Laplace's equation (Eq. 5). The microwell's diameter and thickness are  $100 \mu\text{m}$  and  $10 \mu\text{m}$ , respectively.  $V_0 = 10 \text{ V}$ . (c) Numerical solution of DEP force exerted on a model mammalian cell, where magnitudes and directions of the force vectors are represented by a color map and arrows, respectively. Contours represent electrical potential ( $\Delta V = 0.5 \text{ V}$ ).

oxide (ITO)-coated glass slides were purchased from Delta Technologies (Stillwater, MN). PDMS prepolymer and curing agent (Sylgard 184) were obtained from Dow Corning (Midland, MI). SU-8 photoresist and SU-8 developer were purchased from MicroChem

(Newton, MA). Knock-Out Dulbecco's modified Eagle's medium (KO-DMEM), phosphate buffered saline (PBS), fibronectin, trypsin, L-glutamine, penicillin/streptomycin, non-essential amino acids (NEAA), and LIVE/DEAD viability/cytotoxicity kit were purchased

from Invitrogen (Carlsbad, CA). Fetal bovine serum (FBS) was purchased from HyClone (Logan, UT). Leukemia inhibitory factor (LIF) was purchased from Millipore (Temecula, CA). 7-Aminoactinomycin D (7-AAD) was purchased from BD Biosciences (San Jose, CA). Polystyrene microspheres (25  $\mu\text{m}$  mean diameter) were purchased from Duke Scientific (Palo Alto, CA).

#### Finite-Element Method Analysis

A commercially available finite-element solver, COMSOL Multiphysics (COMSOL, Stockholm, Sweden), was used to solve the Laplace's equation (Eq. 5) for the electric field modulated by the PEG microwells. With obtained electric field, theoretical DEP force on a model mammalian cell was computed from Eq. 1.

#### Fabrication of PEG Microwells and Microfluidic Systems

PEG microwells were made on ITO glass slides using PDMS mold-based soft lithography. The mold master was fabricated by photolithography of SU-8 photoresist on a silicon wafer. Prior to application of PDMS pre-polymer, the master was treated with vapor-phase (tridecafluoro-1,1,2,2-tetrahydrooctyl) trichlorosilane for 15 min in a vacuum desiccator to prevent bonding between the master and the cured PDMS mold. 60 g of the PDMS mixture (pre-polymer 10: curing agent 1) was applied on the master and cured for 2 h at 65  $^{\circ}\text{C}$ . The PDMS mold was then peeled from the master and cut into each piece. Inlet and outlet holes were punched through the mold. Similar to the mold master, surface of the PDMS mold was passivated with vapor-phase (tridecafluoro-1,1,2,2-tetrahydrooctyl) trichlorosilane.

PEG microwells were fabricated on an ITO glass slide which served as the bottom plate of the microfluidic channel as well as the bottom electrode. First, ITO surface was functionalized with acrylate groups for covalent bonding with PEG-DA structures (Fig. 3a). ITO glass slides were cleaned with solvent wash (acetone, methanol, and isopropanol), rinsed with deionized (DI) water, and dried under nitrogen stream. Cleaned ITO slides were then treated with oxygen plasma (Tegal Plasma Asher, Tegal, Petaluma, CA) for 10 min and immediately incubated in a toluene solution containing 3 mM TPA and 1% triethylamine for 1 h. The modified ITO slides were rinsed with toluene, isopropanol, and DI water, followed by nitrogen dry. All slides were stored in a vacuum desiccator until use.

To fabricate the PEG microwells, the PDMS mold was firmly placed on the modified ITO slide, forming a

void space which would define geometries of the PEG layer (Fig. 3b). PEG-DA pre-polymer containing the photo initiator DMPA (1% w/w) was introduced to the void space using capillary force (Fig. 3c). Upon complete filling of the void space by PEG-DA solution, the slide was exposed to 1  $\text{W}/\text{cm}^2$  of UV light for 60 s using a UV spot cure system (EXFO OmniCure S1000, EXFO, Ontario, Canada) (Fig. 3d). After removal of the PDMS mold, excess volume of PEG-DA was trimmed to complete fabrication of PEG hydrogel microwell layer (Fig. 3e). The PEG microwell chip was incubated with an ECM protein solution (20  $\mu\text{g}/\text{mL}$  fibronectin in PBS) for 30 min, followed by DI water rinse and nitrogen dry (Fig. 3f). The coated chip was typically used within a day.

The top assembly of the microchannel was fabricated by similar molding of PDMS. First, a small piece of clean ITO slides (approximately 10 mm  $\times$  10 mm) were modified with 10-undecenyl trimethoxysilane (3 mM solution in toluene containing 1% triethylamine) following the same protocol as for the TPA modification. This modification rendered vinyl groups, allowing for formation of covalent linking to PDMS microchannel during the curing process. After electrical wiring (i.e., a conductive copper tape) was attached, this ITO piece was placed on the SU-8 channel mold master (Fig. 3g), and PDMS pre-polymer was poured and cured for 2 h at 65  $^{\circ}\text{C}$  (Fig. 3h). The PDMS channel was then peeled from the master and cut into

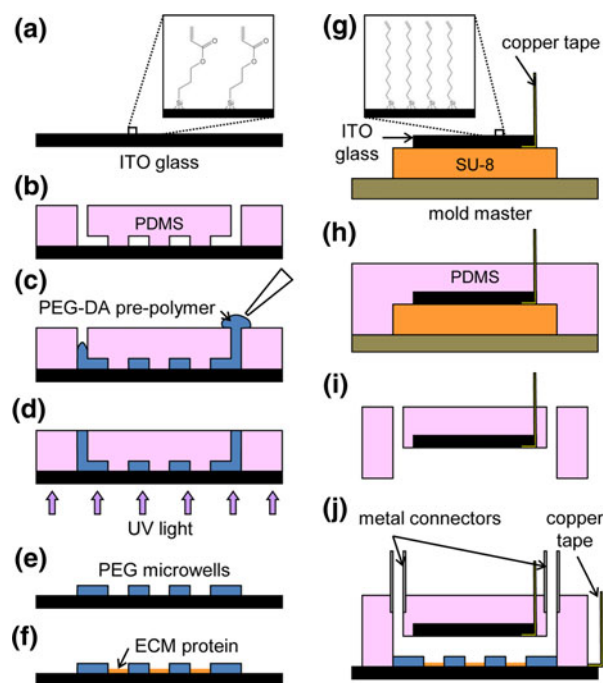


**FIGURE 3.** Fabrication of a microfluidic channel with an embedded PEG microwell array and integrated ITO electrodes.

each piece. Inlet and outlet holes were punched through the mold (Fig. 3i). Finally fabrication of the microfluidic channel system was completed by assembling the top PDMS microchannel and the bottom ITO slide with PEG microwells and inserting stainless steel coupling tubes into the channel inlet and outlet (Fig. 3j).

### *Cell Culture and Preparation*

Murine ES cells LW1<sup>24</sup> were routinely cultured on irradiated mouse embryonic fibroblast (MEF) cells in Knock-Out DMEM supplemented with 15% FBS, 1000 U/mL leukemia inhibitory factor, 2 mM L-glutamine, penicillin, streptomycin, 0.1 mM non-essential amino acids, and 100  $\mu$ M  $\beta$ -mercaptoethanol. This culture medium is referred as ES medium throughout this article. ES cells were fed with fresh medium every other day. Before formation of cell arrays, ES cells were transferred to gelatin-coated plates and cultured for two passages to eliminate residual MEF cells from culture. All cultures were maintained in a 37 °C humidified incubator supplemented with 5% CO<sub>2</sub>.

Immediately prior to cell patterning experiments, ES cells were trypsinized, resuspended in an isoosmotic, low-conductivity buffer solution (LCB), and kept on ice. LCB was DI water-based solution containing 10 mM HEPES, 0.1 mM calcium chloride, 59 mM D-glucose, and 236 mM sucrose,<sup>3</sup> and its pH was adjusted to 7.35 by NaOH<sub>aq</sub>, with a final conductivity of 0.020 S/m.

### *Dielectrophoretic Patterning of ES Cells*

The assembled microchannel was mounted on a Leica DMIRB inverted fluorescence microscope (Leica Microsystems, Bannockburn, IL) equipped with a CoolSNAP HQ CCD camera (Photometrics, Tucson, AZ) for image recoding. During the patterning process and the following culture period, temperature (37 °C) and CO<sub>2</sub> level (5%) were maintained using a stage-top incubator system (Incubator L, CTI-Controller 3700, Tempcontrol 37-2 digital, and Heating Stage, all from PeCon GmbH, Erbach, Germany).

The microchannel was first fed with ethanol to remove air bubbles, followed by complete replacement with LCB. All fluidic flow was operated by a peristaltic pump (Instech Laboratories, Plymouth Meeting, PA) controlled by LabVIEW software (National Instruments, Austin, TX). Cell suspension was introduced into the channel and, when the cells reached the microwell array section, AC electrical potential (20  $V_{pp}$  at 10 MHz) was applied between the electrodes by a

function generator (33120A, Hewlett-Packard, Palo Alto, CA) to initiate the DEP cell patterning process. Upon completion of patterning, AC potential was removed, and LCB was replaced with fresh ES medium described above. Environmental control (37 °C temperature and 5% CO<sub>2</sub>) and continuous feeding of the medium were continued until experiments were terminated.

### *Cell Viability Assay*

Two types for cell viability tests were used in this study. First, effects of LCB on the viability of mES cells were investigated by flow cytometry with 7-AAD staining. Briefly, cells maintained under the standard culture condition were dissociated into single cells using trypsin, centrifuged for 5 min, resuspended in LCB, and kept either on ice or at room temperature for 30 min. A portion of cells were then transferred to adhesion culture with the ES medium on a fibronectin-coated multi-well plate for later analyses. The remaining portion was collected, centrifuged for 5 min, resuspended in 350  $\mu$ L of Hank's Buffered Salt Solution (HBSS) containing 4% serum, incubated with 7  $\mu$ L of 7-AAD solution for 5 min, and kept on ice before FACS analysis. Non-viable cells are readily stained by 7-AAD, a nucleic acid dye, penetrating through the compromised cell membrane, while viable cells remain unstained. Cell viability data was acquired and analyzed with BD FACS Canto II Flow Cytometry System (BD Biosciences, San Jose, CA). To determine the gating for non-viable population, a mixture of viable ES cells and non-viable ES cells, prepared by incubating with 0.1% saponin in D-PBS for 10 min, was used to define gating for live cell population as shown in Fig. 4. The mES cells transferred to and maintained on the adhesion culture were similarly analyzed after 24 h and 72 h counting from the 30-min incubation in LCB.

Viability of cells after patterning was measured using Invitrogen's LIVE/DEAD viability/cytotoxicity kit (Cat. No. L3224) by following supplied instructions. Briefly, the patterned cells were incubated for 30 min in 5  $\mu$ M calcein AM and 5  $\mu$ M ethidium homodimer-1 (EthD-1) in D-PBS. Calcein AM is a cell-permeant dye that is enzymatically converted to the intensely green fluorescent calcein in viable cells, while EthD-1 can only enter cells through compromised membrane of non-viable cells and stain red after binding to the nucleic acids. Fluorescence images of the stained cells were captured using the inverted fluorescence microscope and the CCD camera described above.

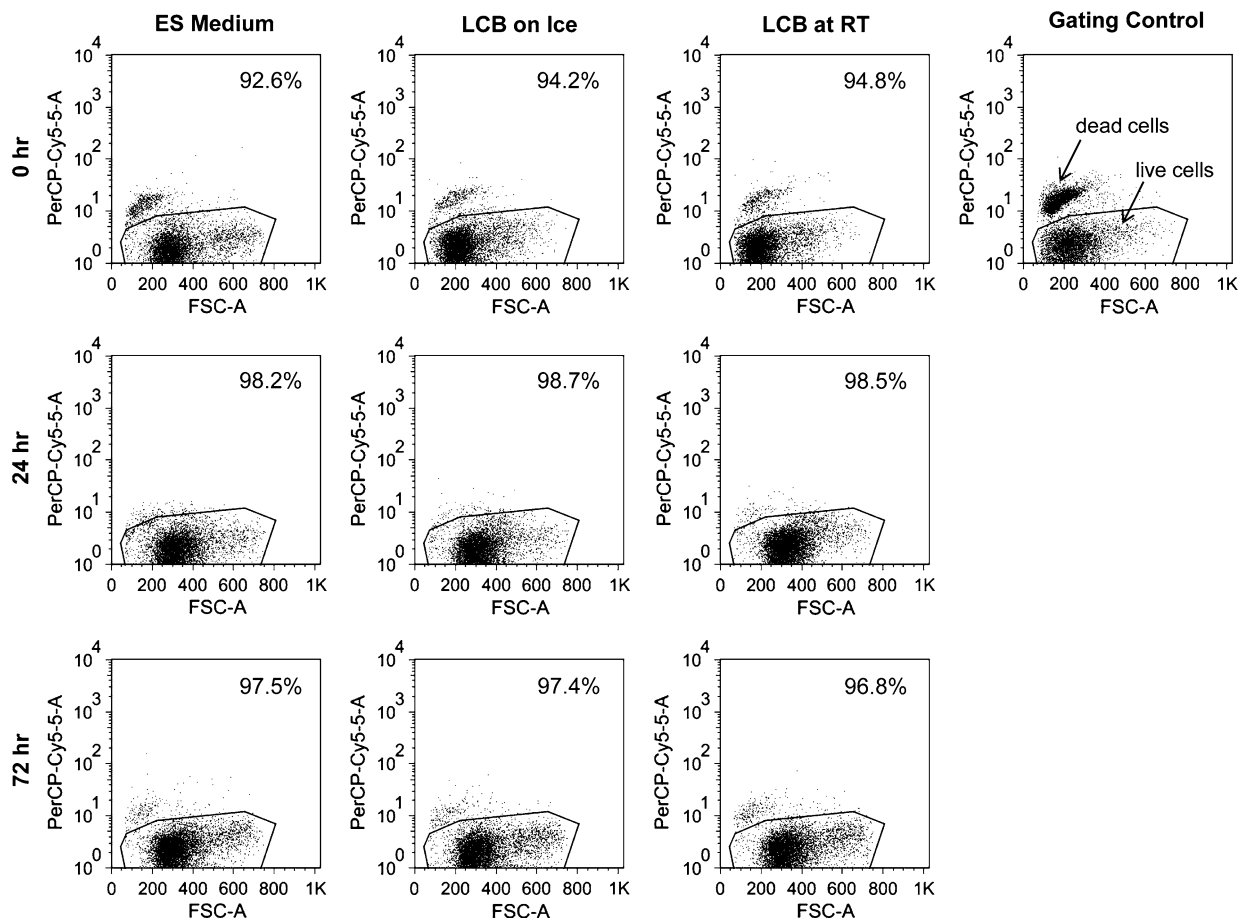


**FIGURE 4.** Flow cytometry analysis of mES cell viability after a 30-min incubation in LCB. Routinely cultured mES cells were trypsinized, centrifuged, resuspended in LCB, and kept for 30 min either on ice or at room temperature (RT). Cells were then transferred to adhesion culture on fibronectin-coated plates supplemented with the ES medium, and maintained in a tissue culture incubator. Cells were sampled immediately after the 30-min LCB incubation and 24 h and 72 h thereafter, and analyzed for viability using 7-AAD staining. An equal mixture of healthy and dead mES cells was used to define a gating for the live population (“Gating Control”). Routinely maintained mES cells without LCB incubation were used as a positive control (“ES Medium”). Based on percentage of viable cells, no adverse effects on cell viability due to 30-min LCB incubation were observed. FSC-A: forward scattering area; PerCP-Cy5-5-A: light intensity corresponding to 7-AAD’s emission.

## RESULTS AND DISCUSSIONS

### *Finite-Element Method Analysis*

According to published experimental work,<sup>31</sup> dielectric constant of PEG-DA is approximately 10 in the frequency range between 1 Hz and 10 MHz. Conductivity of PEG-DA was also estimated from experimental data available in the literature.<sup>4,10</sup> However, the conductivity of PEG-DA was not necessary for the current analysis as either of the Laplace’s equations nor the CM factor required this value. The electrical properties of the LCB and mammalian cells were adapted from the literature.<sup>2,15</sup> List of materials’ conductivity and permittivity are summarized in Table 1.

The estimated DEP force field on the model cell around a PEG microwell (100  $\mu\text{m}$  diameter and 10  $\mu\text{m}$  thickness) is shown in Fig. 2c. Distribution of the DEP

**TABLE 1.** Electrical properties of materials and cell components.

	Conductivity $\sigma$ ( $\text{Sm}^{-1}$ )	Dielectric constant $\epsilon$ ( $\epsilon_0 = 8.854 \times 10^{-12} \text{ Fm}^{-1}$ )
Material		
LCB	0.020	80
PEG-DA	$10^{-5}$ – $10^{-7}$	10
Cell component		
Cell membrane	$3 \times 10^{-6}$	8
Cytoplasm	0.5	50

force, where arrows and the color map indicate direction and magnitude of the force, respectively, predicted movement of all viable cells into the microwell. It was also anticipated that the cells will be primarily attracted to the edges where maximum DEP force is available.

### Viability Tests of Cells Incubated in LCB

Positive DEP manipulation of the cells requires a low-conductivity environment. We thus use LCB while patterning the cells and later replace it with the ES medium. In our protocol, mES cells are typically exposed to LCB for less than 30 min. To evaluate effects of LCB on the viability of cells, we first incubated mES cells in LCB for 30 min and measured the viability using 7-AAD staining and flow cytometry at three different time points: immediately after the incubation (0 h), after 24-h and 72-h incubations in the ES medium. As shown in Fig. 4, 30-min incubations in LCB either on ice or at room temperature (RT) did not compromise apparent cell viability. This result indicates that the necessary exposure to LCB during DEP patterning has minimal effects on the immediate and subsequent cell viability.

### Cell Patterning without an External Flow

We first demonstrated patterning of polystyrene beads (negative DEP particles) and mES cells (positive DEP particles) without an external flow. Once particles

were introduced to the microwell array section, the flow was stopped and DEP patterning was initiated by applying an AC potential ( $20 V_{pp}$  at 10 MHz). As shown in Fig. 5, 92% of mES cells were trapped in the microwells within 10 s, while 88% of polystyrene beads were pushed away from the wells by negative DEP force, forming a rectangular grid pattern which corresponded to local minima of the electric field strength. The 8% of mES cells remained outside of the wells are likely due to spontaneous adhesion of the cells to the substrate. On the other hand, it seems that 12% of the beads remained inside the wells because of the local minimum of the electric field strength at the center of the wells. This set of experiments proved that electric field was indeed modulated by the PEG microwells, forming positive DEP trap arrays as designed.

### Cell Patterning with an External Flow

After successful entrapment of mES cells without an external flow, we demonstrated DEP patterning of mES cells in a continuous flow (flow rate:  $3 \mu\text{L}/\text{min}$ ) with two different cell seeding density:  $10^6$  cells/mL

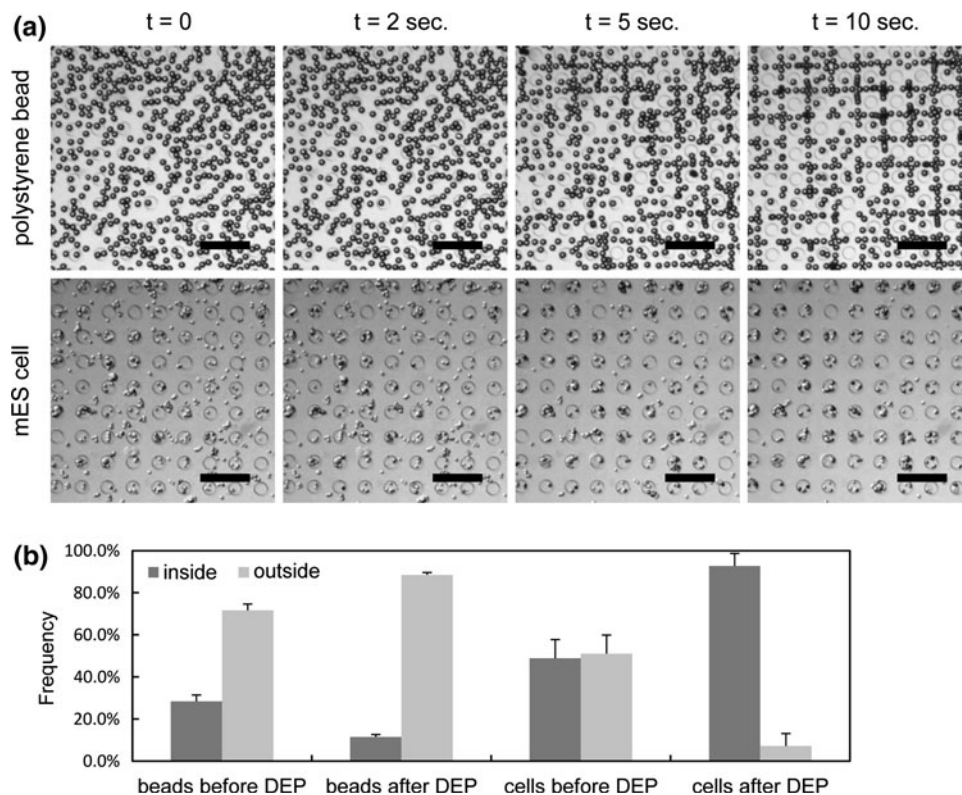


**FIGURE 5.** DEP manipulation of polystyrene beads (negative DEP) and mES cells (positive DEP) without an external flow under low-conductivity environments. (a) Polystyrene beads ( $25 \mu\text{m}$ ) and mES cells demonstrated opposite movements; the polystyrene beads experienced negative DEP forces and the majority moved to regions of weak electric field, while almost all mES cells experiencing positive DEP forces were trapped in the microwells where electric field is strong. Scale bars:  $200 \mu\text{m}$ . (b) Frequency of the polystyrene beads and mES cells found inside and outside of the microwells before and after DEP manipulations. For each sample, the error bar indicates the standard deviation calculated from three data sets.



and  $10^7$  cells/mL. At the lower cell seeding density, majority of cells in the field of view immediately responded to the applied electric field and moved to the microwells within 1 s after initiation of DEP manipulation (Fig. 6a). On the other hand, due to a small number of incoming cells, filling of the microwells required a longer time. At a higher cell seeding density, initial response of individual cells was relatively slow. Nevertheless, a larger number of incoming cells allowed for almost complete filling of the microwells within 25 s (Fig. 6b).

In another set of experiments, continuous operation for a period of a few minutes allowed for complete filling of the microwells with mES cells and subsequent formation of uniform monolayer patterns upon removal of the AC potential and a gentle rinsing step. After replacement of LCB with the fresh ES medium and 1 day of continuous culture, a high viability of the patterned cells (>95% live) was confirmed by the live/

dead staining assay (Fig. 6c). This positive DEP-based patterning approach requires cells to be exposed to environments that are not common for routine tissue culture, i.e., a low-conductivity medium and a highly non-uniform electric field. Thus, typical patterning operations are completed in a relatively short time so that cells are only exposed to LCB for at most 30 min and the electric field for 3 min or less. While this strategy allows for survival of most mES cells during the patterning process, long-term effects on cell growth and differentiation need to be investigated in future work.

#### *Device Development and Operations*

In order to develop the proposed microfluidic device, various key fabrication techniques were adapted or developed. The most critical one among them was to engineer interfaces so that secure covalent

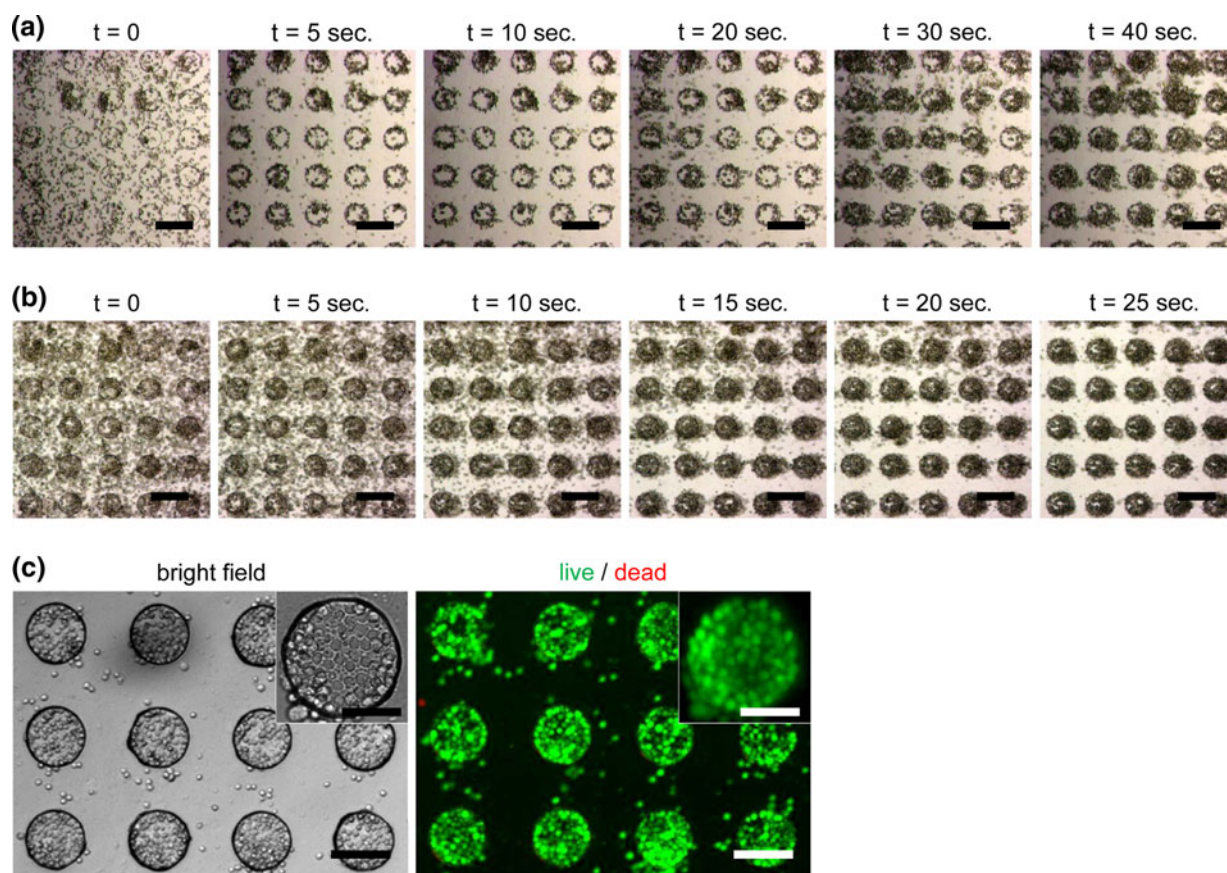


**FIGURE 6.** DEP patterning of mES cells with an external flow, demonstrating quick capture and assembly of the cells and formation of a viable homogeneous cell array. (a) At a lower cell seeding density ( $10^6$  cells/mL), majority of cells in the field of view were trapped in the wells within 1 s after initiation of DEP manipulation. Due to smaller number of incoming cells, filling of microwells required a longer time. Applied AC potential was  $20V_{pp}$  at 10 MHz. Flow direction and rate were from left to right and  $3 \mu\text{L}/\text{min}$  (approximately an average speed of  $250 \mu\text{m}/\text{s}$ ), respectively. (b) At a higher cell seeding density ( $10^7$  cells/mL), initial response of individual cells were relatively slow. Nevertheless, a larger number of incoming cells allowed for almost complete filling of microwells within 25 s. Performed under the same experimental conditions as (a) except for the cell seeding density. (c) Bright field and fluorescent images of the patterned mES cells stained using the LIVE/DEAD kit after 1 day from the DEP patterning operation. Scale bars:  $200 \mu\text{m}$  (a, b),  $100 \mu\text{m}$  (c), and  $50 \mu\text{m}$  (insets of c), respectively.

bonds were formed between ITO and PEG-DA as well as between glass and PDMS. On glass or silicon substrates, PEG-DA hydrogel is typically immobilized by silane modification of surface hydroxyl groups with acrylate-terminated trichloro- or trimethoxy-silane (e.g., TPA) and subsequent free radical polymerization of PEG-DA pre-polymers.<sup>22,27,33,37</sup> While this is a robust approach on glass and silicon substrates, very few reported the same modification strategy on ITO. In our study, only the trimethoxy silane (i.e., TPA) successfully rendered reliable covalent linking on ITO. 3-(Trichlorosilyl)propyl acrylate, on the other hand, noticeably eroded the ITO surface and did not yield stable coupling with PEG-DA hydrogel. The other key development was functionalization of the top electrode ITO glass piece with vinyl group so that covalent link would be formed between the top electrode and PDMS channel during the curing process of PDMS (Fig. 3h). We tested two trimethoxysilane molecules with a vinyl terminal, including 10-undecenyltrimethoxysilane ( $C_{14}H_{30}O_3Si$ ) and vinyltrimethoxysilane ( $C_5H_{12}O_3Si$ ), along with controls (glass and ITO with or without

plasma treatment) and found that only the substrates treated with 10-undecenyltrimethoxysilane successfully yielded stable adhesion between PDMS and both ITO and glass. Although detailed investigation is required, it is likely that the long carbon chains of this silane molecule improved chances of polymerization between two vinyl groups from the silane monolayer on ITO surface and the PDMS pre-polymer. To our knowledge, this is the first demonstration of a PDMS channel with a literally embedded ITO glass electrode. Due to ease of both fabrication and subsequent assembly with a bottom electrode plate, this technique could provide a convenient way of fabricating microfluidic systems with top and bottom parallel electrodes.<sup>3,8</sup>

In this study, we found that available DEP force significantly changed within the frequency range of 1–10 MHz (Fig. 7a). This frequency range is widely used for positive DEP manipulation of cells by metal electrode-based devices because the CM factor peaks within this range, offering the maximum DEP force (Fig. 7b). However, an insulator-based electrode array in the current system is more sensitive to the operation

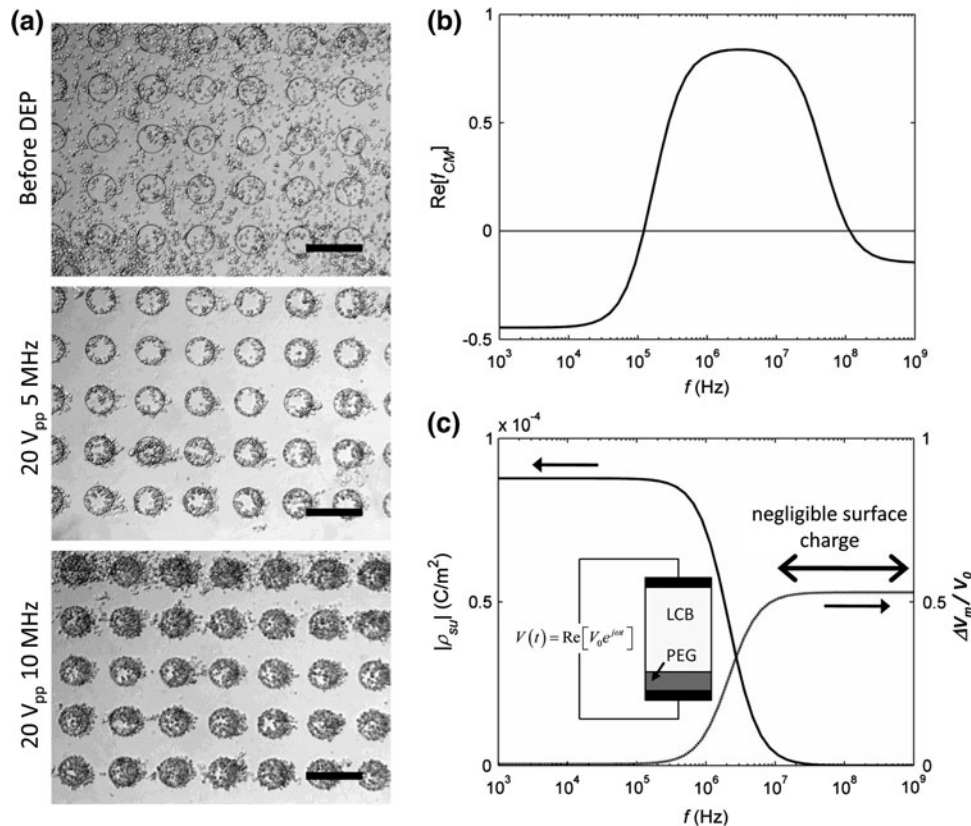


**FIGURE 7.** Frequency dependence of DEP force and patterning efficiency. (a) Significant reduction of positive DEP forces on mES cells was observed at frequencies below 10 MHz. Seeding density:  $10^6$  cells/mL and flow rate:  $3 \mu\text{L}/\text{min}$ . (b) Frequency dependence of the CM factor having a wide peak band between 1 MHz and 10 MHz. (c) Interfacial charge accumulation and corresponding potential drop ( $\Delta V_m$ ) across the medium phase (i.e., LCB) was estimated by using a simple one-dimensional model (see inset). This model indicates that the interfacial charges are no longer negligible below 10 MHz and causes significant loss of  $\Delta V_m$ , meaning non-uniform electric fields required for DEP manipulation are equally attenuated. Scale bars:  $200 \mu\text{m}$ .

frequency due to non-negligible charge accumulation at the interface between the solution and PEG and subsequent potential drop across the PEG layer at frequencies below 10 MHz (Fig. 7c, see Appendix). Therefore, this device must be operated at ~10 MHz in order to maximize contributions from both the CM factor and  $\nabla|E_{\text{rms}}|^2$  in Eq. 1.

### Hydrogel Materials Selection

In this study, PEG-DA 258 (Mn ~ 258) was chosen as the building material of the microwells. It is known that the non-fouling property of PEG-based hydrogels improves with the molecular weight (MW) of the pre-polymer PEG-DA. In a recent extensive study by Moeller *et al.*,<sup>27</sup> microwells made of PEG-DA 258 suffered from significant protein absorption and cell adhesion compared with microwells made of larger MW PEG-DAs such as PEG-DA 575 (Mn ~ 575) and PEG-DA 1000 (Mn ~ 1000). This relatively low non-fouling property led to outgrowth of embryoid bodies (EBs) and poor retrieval from the microwells. On the other hand, hydrogels made of higher MW PEGs undergo significant swelling under aqueous conditions,<sup>26</sup> leading to poor structural stability of the microwells anchored on substrates.<sup>27</sup> Consequently, pre-polymer solutions of the above-mentioned PEG-DA 575 and 1000 needed to be significantly diluted (e.g., 20% PEG-DA: 80% PBS) so that relative amount of swelling upon full hydration was small enough.<sup>27</sup> In this study, in addition to providing non-fouling surfaces and physical structures, PEG microwells play a key role as a dielectric component, creating a strong non-uniform electric field for actively trapping mES cells. Hence, the use of diluted (or pre-hydrated) high MW PEG-DA which lowers the relative dielectric constant of the microwells is not desirable. Consequently, PEG-DA 258 seems to be the best compromise for the proposed application at this moment. Beyond PEG-based hydrogels, more robust polymer materials such as polyacrylamide<sup>28</sup> and PDMS<sup>42</sup> recently demonstrated excellent non-fouling properties, and they might serve as an excellent substitute material for the current application in the future.

## CONCLUSION

We have developed a novel microfluidic platform with an embedded array of PEG-DA microwells for actively patterning mES cells by positive DEP. The uniqueness of our approach lies in the use of surface-engineered PEG-DA hydrogel not only as a typical non-fouling layer, but also as a key electrical component to define electrical energy landscapes within a

microfluidic system. Due to dielectric properties of the PEG microwells, an applied AC potential by ITO electrodes creates a strong non-uniform electric field around the microwells, forming positive DEP traps for mammalian cells in a low-conductivity environment. Positive DEP-based patterning in this platform allowed fast trapping and patterning of mES cells in the microwells within tens of seconds. Captured cells subsequently formed homogeneous monolayer and remained mostly viable as confirmed by the live/dead assay. Furthermore, as evidenced in Figs. 5 and 6, the positive DEP traps successfully collected the majority of the cells available in the field. Therefore, total consumption of cells could be minimized with this approach when compared to conventional surface-based patterning methods where a large number of cells are required and eventually wasted. In addition, this efficient patterning method can be easily applied to the patterning of other types of mammalian cells. Due to the simplicity of the device design and operation, this technology is readily scalable and could facilitate manufacturing of large-scale cell arrays.

## APPENDIX

### CM Factor Calculation

In order to calculate the CM factor in Eq. 2, a mammalian cell was modeled as a spherical concentric dielectric shell with an outer radius  $r$  ( $= 4.0 \times 10^{-6}$  m) and membrane thickness  $d_{\text{mem}}$  ( $= 8.0 \times 10^{-9}$  m) having shell permittivity  $\epsilon_{\text{mem}}^*$  ( $= \epsilon_{\text{mem}} - j\sigma_{\text{mem}}/\omega$ ) and core permittivity  $\epsilon_{\text{cyto}}^*$  ( $= \epsilon_{\text{cyto}} - j\sigma_{\text{cyto}}/\omega$ )<sup>21</sup>:

$$\epsilon_p^* = \epsilon_{\text{mem}}^* \frac{r^3(\epsilon_{\text{cyto}}^* + 2\epsilon_{\text{mem}}^*) + 2(r - d_{\text{mem}})^3(\epsilon_{\text{cyto}}^* - \epsilon_{\text{mem}}^*)}{r^3(\epsilon_{\text{cyto}}^* + 2\epsilon_{\text{mem}}^*) - (r - d_{\text{mem}})^3(\epsilon_{\text{cyto}}^* - \epsilon_{\text{mem}}^*)} \quad (7)$$

The CM factor was then calculated from Eqs. 2 and 7 using MATLAB (MathWorks, Matick, MA). Parameter values used were adapted from the published literature<sup>15</sup> and listed in Table 1.

### Interfacial Charge Accumulation

Positive DEP manipulation of mammalian cells in a low-conductivity environment is typically operated at a frequency range 1–10 MHz where the CM factor peaks, maximizing available DEP force. Nevertheless, in this experimental study, significant loss of attractive force was observed at frequencies below 10 MHz. This is because the assigned interfacial condition in Fig. 2 (i.e., no charge accumulation at interface between the

PEG-DA and LCB) is no longer valid at these frequencies. At a lower frequency, charges can transfer fast enough to accumulate at the interface, counteracting the electric field generated by the applied AC potential. In other words, accumulated charges effectively reduce potential drop across the fluid domain and subsequently minimize magnitude of non-uniform electric field required for DEP forces (see Eq. 1).

We attempted to estimate the interfacial charge accumulation  $\rho_{su}$  by assuming a simple model system shown in the inset of Fig. 7c and using a corresponding analytical solution<sup>18</sup>:

$$\rho_{su} = \text{Re} \left[ \frac{(\epsilon_a \sigma_b - \epsilon_b \sigma_a) V_0}{(h_b \sigma_a + h_a \sigma_b) + j\omega(h_b \epsilon_a + h_a \epsilon_b)} e^{j\omega t} \right], \quad (8)$$

where  $\sigma$ ,  $\epsilon$ , and  $h$  are conductivity, permittivity, and height, respectively, and subscripts  $a$  and  $b$  indicate corresponding domains, medium and PEG-DA, respectively.

### ACKNOWLEDGMENTS

This study is supported by the Center for Cell Control (1PN2 ey018228) through the NIH Roadmap for Nanomedicine, and the Center for Scalable and Integrated Nanomanufacturing (SINAM) under National Science Foundation (CMMI-0751621).

### OPEN ACCESS

This article is distributed under the terms of the Creative Commons Attribution Noncommercial License which permits any noncommercial use, distribution, and reproduction in any medium, provided the original author(s) and source are credited.

### REFERENCES

- <sup>1</sup>Albrecht, D. R., V. L. Tsang, R. L. Sah, and S. N. Bhatia. Photo- and electropatterning of hydrogel-encapsulated living cell arrays. *Lab Chip* 5(1):111–118, 2005.
- <sup>2</sup>Albrecht, D. R., G. H. Underhill, T. B. Wassermann, R. L. Sah, and S. N. Bhatia. Probing the role of multicellular organization in three-dimensional microenvironments. *Nat. Methods* 3(5):369–375, 2006.
- <sup>3</sup>Albrecht, D. R., G. H. Underhill, A. Mendelson, and S. N. Bhatia. Multiphase electropatterning of cells and biomaterials. *Lab Chip* 7(6):702–709, 2007.
- <sup>4</sup>Alig, I., S. A. Dudkin, W. Jenninger, and M. Marzantowicz. Ac conductivity and dielectric permittivity of poly(ethylene glycol) during crystallization: percolation picture. *Polymer* 47(5):1722–1731, 2006.
- <sup>5</sup>Banerjee, P., and A. K. Bhunia. Mammalian cell-based biosensors for pathogens and toxins. *Trends Biotechnol.* 27(3):179–188, 2009.
- <sup>6</sup>Bhatia, S. N., M. L. Yarmush, and M. Toner. Controlling cell interactions by micropatterning in co-cultures: hepatocytes and 3T3 fibroblasts. *J. Biomed. Mater. Res.* 34(2): 189–199, 1997.
- <sup>7</sup>Chen, C. S., M. Mrksich, S. Huang, G. M. Whitesides, and D. E. Ingber. Geometric control of cell life and death. *Science* 276(5317):1425–1428, 1997.
- <sup>8</sup>Chiou, P. Y., A. T. Ohta, and M. C. Wu. Massively parallel manipulation of single cells and microparticles using optical images. *Nature* 436(7049):370–372, 2005.
- <sup>9</sup>Chung, B. G., L. F. Kang, and A. Khademhosseini. Micro- and nanoscale technologies for tissue engineering and drug discovery applications. *Expert. Opin. Drug Discov.* 2(12): 1653–1668, 2007.
- <sup>10</sup>Craig, D. Q. M., J. M. Newton, and R. M. Hill. An investigation into the low-frequency dielectric response of polyethylene glycols. *J. Mater. Sci.* 28(2):405–410, 1993.
- <sup>11</sup>Cummings, E. B., and A. K. Singh. Dielectrophoresis in microchips containing arrays of insulating posts: theoretical and experimental results. *Anal. Chem.* 75(18):4724–4731, 2003.
- <sup>12</sup>Falconnet, D., G. Csucs, H. M. Grandin, and M. Textor. Surface engineering approaches to micropattern surfaces for cell-based assays. *Biomaterials* 27(16):3044–3063, 2006.
- <sup>13</sup>Folch, A., and M. Toner. Microengineering of cellular interactions. *Annu. Rev. Biomed. Eng.* 2:227–256, 2000.
- <sup>14</sup>Folch, A., B. H. Jo, O. Hurtado, D. J. Beebe, and M. Toner. Microfabricated elastomeric stencils for micropatterning cell cultures. *J. Biomed. Mater. Res.* 52(2):346–353, 2000.
- <sup>15</sup>Glasser, H., and G. Fuhr. Cultivation of cells under strong ac-electric field—differentiation between heating and transmembrane potential effects. *Bioelectrochem. Bioenerg.* 47(2):301–310, 1998.
- <sup>16</sup>Gray, D. S., J. L. Tan, J. Voldman, and C. S. Chen. Dielectrophoretic registration of living cells to a microelectrode array. *Biosens. Bioelectron.* 19(7):771–780, 2004.
- <sup>17</sup>Green, N. G., A. Ramos, and H. Morgan. Numerical solution of the dielectrophoretic and travelling wave forces for interdigitated electrode arrays using the finite element method. *J. Electrostat.* 56(2):235–254, 2002.
- <sup>18</sup>Haus, H. A., and J. R. Melcher. *Electromagnetic Fields and Energy*. Englewood Cliffs, NJ: Prentice-Hall, 1989.
- <sup>19</sup>Healy, K. E., B. Lom, and P. E. Hockberger. Spatial-distribution of mammalian-cells dictated by material surface-chemistry. *Biotechnol. Bioeng.* 43(8):792–800, 1994.
- <sup>20</sup>Irimia, D., and J. O. M. Karlsson. Development of a cell patterning technique using poly(ethylene glycol) disilane. *Biomed. Microdevices* 5(3):185–194, 2003.
- <sup>21</sup>Jones, T. B. *Electromechanics of Particles*. Cambridge: Cambridge University Press, 1995.
- <sup>22</sup>Khademhosseini, A., S. Jon, K. Y. Suh, T. N. T. Tran, G. Eng, J. Yeh, J. Seong, and R. Langer. Direct patterning of protein- and cell-resistant polymeric monolayers and microstructures. *Adv. Mater.* 15(23):1995–2000, 2003.
- <sup>23</sup>Khademhosseini, A., G. Eng, J. Yeh, P. A. Kucharczyk, R. Langer, G. Vunjak-Novakovic, and M. Radisic. Microfluidic patterning for fabrication of contractile cardiac organoids. *Biomed. Microdevices* 9(2):149–157, 2007.
- <sup>24</sup>Lesche, R., M. Groszer, J. Gao, Y. Wang, A. Messing, H. Sun, X. Liu, and H. Wu. Cre/LoxP-mediated inactivation of the murine Pten tumor suppressor gene. *Genesis* 32(2):148–149, 2002.
- <sup>25</sup>Li, N., and C. M. Ho. Photolithographic patterning of organosilane monolayer for generating large area

- two-dimensional B lymphocyte arrays. *Lab Chip* 8(12): 2105–2112, 2008.
- <sup>26</sup>Mellott, M. B., K. Searcy, and M. V. Pishko. Release of protein from highly cross-linked hydrogels of poly(ethylene glycol) diacrylate fabricated by UV polymerization. *Biomaterials* 22(9):929–941, 2001.
- <sup>27</sup>Moeller, H. C., M. K. Mian, S. Shrivastava, B. G. Chung, and A. Khademhosseini. A microwell array system for stem cell culture. *Biomaterials* 29(6):752–763, 2008.
- <sup>28</sup>Nelson, C. M., S. Raghavan, J. L. Tan, and C. S. Chen. Degradation of micropatterned surfaces by cell-dependent and -independent processes. *Langmuir* 19(5):1493–1499, 2003.
- <sup>29</sup>Pamme, N. Continuous flow separations in microfluidic devices. *Lab Chip* 7(12):1644–1659, 2007.
- <sup>30</sup>Pohl, H. A. Dielectrophoresis: The Behavior of Neutral Matter in Nonuniform Electric Fields. New York: Cambridge University Press, 1978.
- <sup>31</sup>Popielarz, R., C. K. Chiang, R. Nozaki, and J. Obrzut. Dielectric properties of polymer/ferroelectric ceramic composites from 100 Hz to 10 GHz. *Macromolecules* 34(17):5910–5915, 2001.
- <sup>32</sup>Raghavan, S., and C. S. Chen. Micropatterned environments in cell biology. *Adv. Mater.* 16(15):1303–1313, 2004.
- <sup>33</sup>Revzin, A., R. G. Tompkins, and M. Toner. Surface engineering with poly(ethylene glycol) photolithography to create high-density cell arrays on glass. *Langmuir* 19(23): 9855–9862, 2003.
- <sup>34</sup>Roth, E. A., T. Xu, M. Das, C. Gregory, J. J. Hickman, and T. Boland. Inkjet printing for high-throughput cell patterning. *Biomaterials* 25(17):3707–3715, 2004.
- <sup>35</sup>Sanjana, N. E., and S. B. Fuller. A fast flexible ink-jet printing method for patterning dissociated neurons in culture. *J. Neurosci. Methods* 136(2):151–163, 2004.
- <sup>36</sup>Singhvi, R., A. Kumar, G. P. Lopez, G. N. Stephanopoulos, D. I. C. Wang, G. M. Whitesides, and D. E. Ingber. Engineering cell-shape and function. *Science* 264(5159): 696–698, 1994.
- <sup>37</sup>Suh, K. Y., J. Seong, A. Khademhosseini, P. E. Laibinis, and R. Langer. A simple soft lithographic route to fabrication of poly(ethylene glycol) microstructures for protein and cell patterning. *Biomaterials* 25(3):557–563, 2004.
- <sup>38</sup>Takayama, S., J. C. McDonald, E. Ostuni, M. N. Liang, P. J. A. Kenis, R. F. Ismagilov, and G. M. Whitesides. Patterning cells and their environments using multiple laminar fluid flows in capillary networks. *Proc. Natl Acad. Sci. U.S.A.* 96(10):5545–5548, 1999.
- <sup>39</sup>Tourovskaia, A., T. Barber, B. T. Wickes, D. Hirdes, B. Grin, D. G. Castner, K. E. Healy, and A. Folch. Micropatterns of chemisorbed cell adhesion-repellent films using oxygen plasma etching and elastomeric masks. *Langmuir* 19(11):4754–4764, 2003.
- <sup>40</sup>Tsutsui, H., and C. M. Ho. Cell separation by non-inertial force fields in microfluidic systems. *Mech. Res. Commun.* 36(1):92–103, 2009.
- <sup>41</sup>Underhill, G. H., and S. N. Bhatia. High-throughput analysis of signals regulating stem cell fate and function. *Curr. Opin. Chem. Biol.* 11(4):357–366, 2007.
- <sup>42</sup>Valamehr, B., S. J. Jonas, J. Polleux, R. Qiao, S. L. Guo, E. H. Gschweng, B. Stiles, K. Kam, T. J. M. Luo, O. N. Witte, *et al.* Hydrophobic surfaces for enhanced differentiation of embryonic stem cell-derived embryoid bodies. *Proc. Natl Acad. Sci. U.S.A.* 105(38):14459–14464, 2008.
- <sup>43</sup>Wang, X. B., Y. Huang, F. F. Becker, and P. R. C. Gascoyne. A unified theory of dielectrophoresis and traveling-wave dielectrophoresis. *J. Phys. D-Appl. Phys.* 27(7):1571–1574, 1994.
- <sup>44</sup>Whitesides, G. M., E. Ostuni, S. Takayama, X. Y. Jiang, and D. E. Ingber. Soft lithography in biology and biochemistry. *Annu. Rev. Biomed. Eng.* 3:335–373, 2001.